Arab Journal of Nuclear Sciences and Applications

Web site: ajnsa.journals.ekb.eg

(ESNSA)

Sensitivity and Uncertainty Analysis of BEAVRS Benchmark

Mohga Hassan* and Basma Foad

The Egyptian Nuclear and Radiological Regulatory Authority, Cairo, Egypt

The BEAVRS benchmark problem describes detailed information such as the geometry and material specifications to construct a neutronic calculation model of a commercial Pressurized Water Reactor (PWR) core. The benchmark was modified several times; the main purpose of the current study is to investigate the effect of the modifications in the BEAVRS benchmark on sensitivities and uncertainties in cross section that in turn affect the multiplication factors and reactivity coefficients.

The sensitivity coefficients are calculated for k_{eff} due to perturbation in cross-sections using the KSEN card of MCNP6 code for the two cores, where all control rods are in and out. Since MCNP6 cannot calculate uncertainties, the NJOY2021 was used to compute the relative covariance matrices of the cross-sections data library, thereafter, a python script was developed to calculate the uncertainties of k_{eff} as well as sensitivities and uncertainties of reactivity due to the control rods insertion. The results indicate that the uncertainties in reactivities caused by control rods insertion for the BV2 model is greater than the BV1 model, due to the effect of using higher coolant density in the nozzle and support plate structures in addition to the effect of the burnable absorber designs in the BV2 model.

Keywords: *BEAVRS, Sensitivity, Uncertainty, NJOY, MCNP6*

Introduction

The BEAVRS (<u>B</u>enchmark for <u>E</u>valuation and <u>V</u>alidation of <u>R</u>eactor <u>S</u>imulation) benchmark problem provides a detailed specification of the geometries and compositions for the commercial pressurized water reactor (PWR) core power of 3411 MWth. The main purpose of BEAVRS is to allow a comparison of various reactor physics computer codes to construct the neutronic calculation model of the full-core with real plant data, and it was modified several times [1-3]

Some specifications were modified from revision 1 [1] (henceforth BV1) to revision 2 [3] (henceforth BV2). The major update points between BV1 and BV2 cores are the coolant temperatures and densities in the nozzle and support plate structure, the designs of the burnable absorber rod, and the control rods, in addition of some modifications in the upper and lower structures.

In this study, the effect of the above-mentioned design changes on the sensitivity and uncertainty (S&U) due to cross-section perturbations will be investigated. First, the sensitivities and uncertainties of the multiplication factors for the two cores are compared to analyze the effect of using different coolant temperatures and densities in the nozzle and support plate structures in addition to the impact of the burnable absorber design change in BV1 and BV2. Thereafter, the influence of the modifications in the control rods designs is studied by comparing the S&U of reactivities resulting from control rods insertions.

The KSEN card of MCNP6 code [4] is used to calculate sensitivity coefficients of the multiplication factors for BV1 and BV2 cores. To calculate uncertainties, the covariance matrix

---

computed by the NJOY2021 [5] is utilized in the so called sandwish formula [6]. Besides, a python program was written to read the MCNP6 output and the covariance matrices, then performs the sensitivity and uncertainty calculations.

The study is organized as follows: the next section explains the theory and mathematical model used. Section 3 summarizes the differences between BV1 and BV2 models. In Section 4, the MCNP6 model used to simulate both models and calculate the sensitivity coefficients is explained. Section5 illustrates the calculation steps and the relation between MCNP6, NJOY, and the python module. In Section 6, the sensitivity and uncertainty analyses for both models are presented, finally, the conclusion is summarized in Section 7.

Theory
The uncertainty propagation methods can be classified into two approaches [6,7]. The first is the Monte Carlo-based technique (statistical sampling method), which starts by calculating uncertainty by randomly generating possible inputs, then analyzing the distribution of outputs generated by randomly varying inputs. The sampling-based uncertainty is relatively simple, but it is computationally expensive since it needs to run N-times, where N is the sample size. It also has the statistical error which varies as inverse square root with the sample size [8].

The second technique is the sensitivity-based technique [6,7] (deterministic method), it includes two methodologies, the forward (direct) calculation method implemented by varying the inputs one by one and observing the responses, this approach is preferable when there are few input parameters that can vary and many output responses of interest.

The second deterministic method is the adjoint method based on the perturbation theory, in which the sensitivity is calculated using adjoint functions. The perturbation theory will be used in the present work to calculate sensitivity coefficients.

Sensitivity of k_{eff}
In general, the sensitivity coefficient is defined by the relative change of the core characteristic, due to the relative change of the cross-section:

$$S(R) = \frac{dR/R}{d\sigma/\sigma} \qquad (1)$$

Where R is the core characteristics, such as k_{eff}, and σ is the cross-section. The MCNP6.1 offers

two perturbation theory techniques to calculate sensitivities: one is based on the differential operator (PERT card) and another is based on linear perturbation theory using adjoint weighting (KPERT and KSEN cards).

The differential operator technique is based on a Taylor series expansion and works very well for generalized responses with fixed-source problems. In eigenvalue problems, however, the differential operator methodology may produce inaccurate results, because MCNP6 implementation does not account for the perturbation of the fission source distribution [4]. The adjoint weighting perturbation methodology invoked by the KPERT card was designed to investigate changes in k_{eff} as a result of material substitution. While the method, in theory, allows for more general perturbations, it introduces an approximation in the handling of scattering laws that can lead to large and unacceptable deviations in scattering sensitivities.

For this reason, the KSEN capability, which is more accurate, efficient and easier to use than KPERT for this purpose, has been developed. In the present work, the KSEN card is used for calculating MCNP6 sensitivity coefficients. Details of the modelling basis and usage of this function have been reported in previous studies [4, 9].

Sensitivity of reactivity
The reactivity associated with the change in conditions (control rod insertion, temperature, coolant, density, etc.) is defined as:

$$\rho_{1\to2} = \rho_2 - \rho_1 = \frac{1}{k_{eff1}} - \frac{1}{k_{eff2}}$$
(2)

Where k_{eff1} and k_{eff2} are the k-eigenvalues for two different states. In this study, the case where all control rods are out represents state-1 and all control rods in represents state-2.

Williams [10] gave a detailed description of the sensitivity methodology for reactivity responses. He proved that the reactivity sensitivity coefficient, due to change of any arbitrary parameter α, is equal to

$$S_\alpha(\rho) = \frac{\lambda_2 S_{k_2,\alpha} - \lambda_1 S_{k_1,\alpha}}{|\rho_{1\to2}|}, \qquad (3)$$

Where λ_1, λ_2 equals $\frac{1}{k_1}$ and $\frac{1}{k_2}$ are the fundamental lambda Eigenvalues before and after

the change, and $S_{k_1,\alpha}$, $S_{k_2,\alpha}$ are the k-sensitivities for the two states, and $|\rho_{1\rightarrow2}|$ is the absolute value of reactivity change. For isotope i reaction j and energy group g, the sensitivity of reactivity is given by:

$$S_{i,j,g}(\rho) = \frac{\frac{1}{k_{eff2}}.S_{i,j,g}(k_{eff2}) - \frac{1}{k_{eff1}}.S_{i,j,g}(k_{eff1})}{|\rho_{1\rightarrow2}|} \quad (4)$$

Uncertainty calculation method

The sandwish formula is used to calculate the uncertainty or the relative variance of core response 'R'; given by [6,10] :

$$var(R) = \sigma_R^2 = S(R).C.S^T(R) \quad (5)$$

Where S(R) is the sensitivity vector which includes all reactions, nuclides, and energy-groups, the subscript 'T' denotes transpose, and 'C ' is the relative covariance matrix describing cross-section uncertainties and correlations, which are computed using the NJOY2021 code [5]. The relation between the uncertainties of the k-eigenvalues and reactivity responses was investigated in anearlier publication [10] as follows:

$$\sigma_\rho^2 = \left(\frac{\frac{1}{k_{eff1}}}{|\rho_{1\rightarrow2}|}\right)^2 \sigma_{keff1}^2 + \left(\frac{\frac{1}{k_{eff2}}}{|\rho_{1\rightarrow2}|}\right)^2 \sigma_{keff2}^2 - \left(\frac{\frac{2}{k_{eff1}.k_{eff2}}}{\left(\frac{1}{k_{eff1}} - \frac{1}{k_{eff2}}\right)^2}\right)\sigma_{k_{eff1}.k_{eff2}}^2 \quad (6)$$

Where $\sigma_{k_{eff1}}^2$ and $\sigma_{k_{eff2}}^2$ are the relative variance of the k-eigenvalues, and $\sigma_{k_{eff1}.k_{eff2}}^2$ is the relative covariance of the two eigenvalues.

BEAVRS modifications

There are major modifications between BV1 and BV2 cores, which include modifications in the core model which will affect the multiplication factor when all control rods are out of the core. In addition, there are changes in the control rod design that will impact the reactivity coefficients due to control rods insertion. Here are the major updates between the BV1 and BV2 cores, other detailed data are reported in other studies[1-3]:

- The coolant in the nozzle and support plate structures have different temperatures and densities from that in the core. In the BV1 core, the coolant temperature and density were set to 566.5 ^{o}K and 740.6 kg/m^3, respectively. While in the BV2, the coolant temperature and density in the nozzle and support plate were updated to 349.1 ^{o}K and 981.0 kg/m^3 ^{o}K, respectively.

- In the BV2 model, the fuel is lifted by 0.741 cm with no change in active fuel length.

- The main active burnable absorber length did not change, but it was shifted 0.529 cm downwards in BV2.

- The part under the bottom of the burnable absorber rod in BV1 was water in the lower part of the guide tube, while in BV2, the bottom part of the absorber rod is stainless steel (SS) pin introduced as an end plug.

- The plenum region of the burnable absorber was also changed from SS pin in BV1 (33.677 cm) to be replaced in BV2 by two parts; a hollow part that contains air (20.294 cm), directly above burnable absorber rod, then SS pin (10.344cm).

- In the BV2 model, the air which filled the two gaps in the burnable absorber rods had been replaced by helium.

- For the control rods, the control rod material was only Ag-In-Cd (AIC) in BV1. In BV2, the control rods are divided into two parts, an upper part of about 259 cm which has boron carbide (B$_4$C) as an absorber, while the lower part, of about 102 cm, having Silver Indium Cadmium (Ag-In-Cd) absorber.

MCNP Model

A full core model was prepared using the MCNP6.1 code [4]; the BEAVRS model is shown in Figure (1).Multiple runs for the two cores were performed utilizing KSEN card, with all rods out then all rods in. The sensitivity and uncertainty were estimated with all control rods out to evaluate

the effect of using different coolant temperatures and densities in the nozzle and support plate structures in addition to the impact of the burnable absorber and other minor design changes in the upper and lower structures. The influence of

changing the control rods design is investigated by studying the S&U of reactivities resulting from control rods insertions (all control rods are in core).
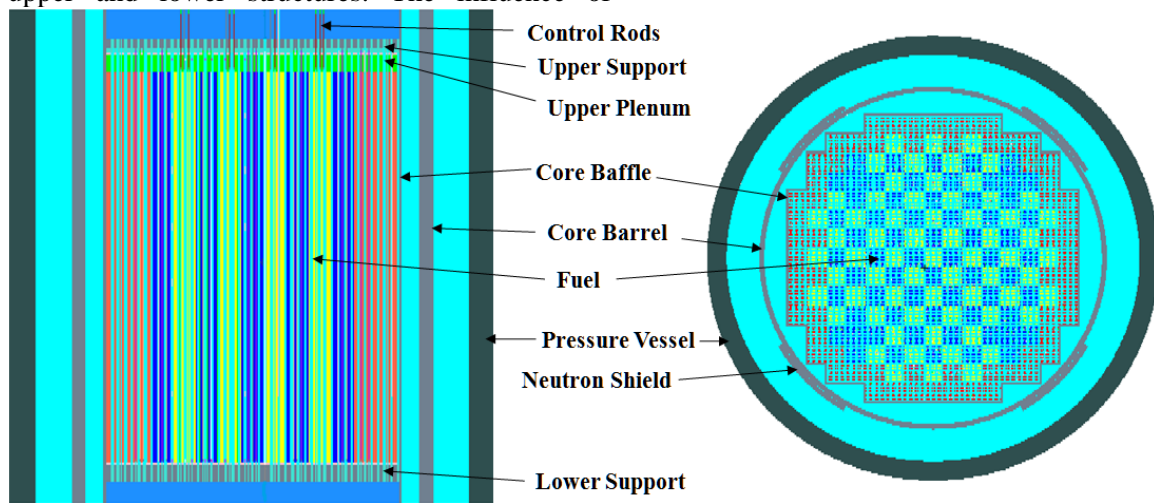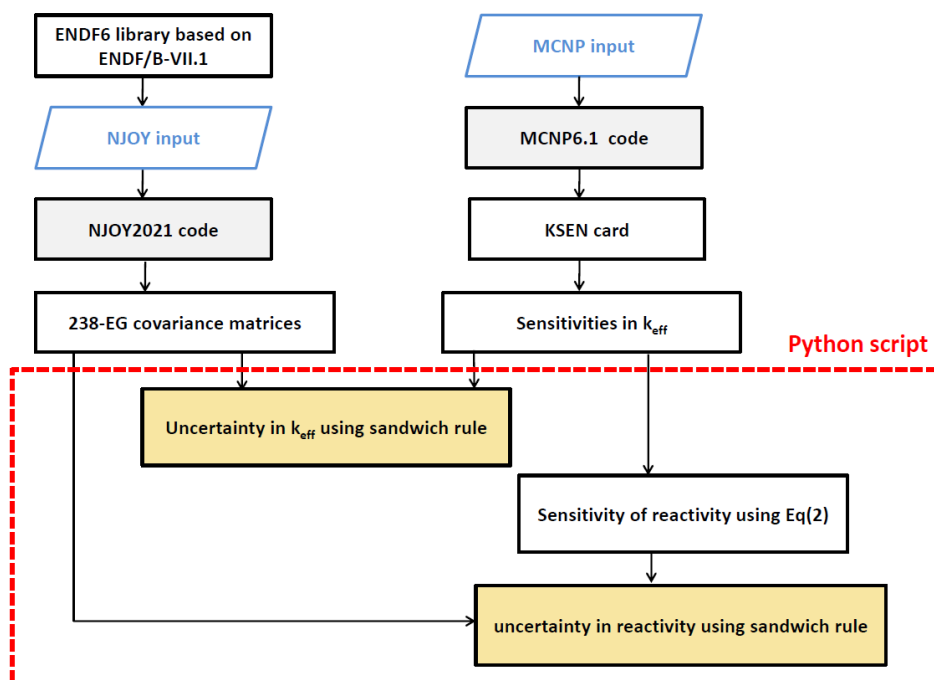

Fig. (1): MCMP model for BEAVRS core

Fig. (2): Flowchart for the calculation steps

Calculation Steps

The overall calculation steps are schematically summarized in Figure 2 as follows:

The 238-energy group structure was used in calculating the sensitivity coefficient, from a minimum of 1×10^{-10} to 20 MeV. The calculations were performed using 175 million neutron histories.

- First, the KSEN card of MCNP6 code is used to calculate sensitivity coefficients of the multiplication factors due to perturbation in ENDF/B-VII.1 cross-section data library for BV1 and BV2 cores, when all control rods are in and out. Sentitivity coefficient is determined for ^{235}U and ^{238}U for fission, capture, elastic and inelastic scattering, fission- ν, fission-χ, and (n,2n) reaction. The main isotopes of water , ^{1}H and ^{16}O were also considered, the calculation included capture and elastic scattering reaction for both isotopes in addition to inelastic scattering for ^{16}O.

- Then, the NJOY2021 code is used to compute the covariance matrices of the ENDF/B-VII.0 cross-section data library.

- Thereafter, a python program is developed to read the k_{eff} sensitivity coefficients calculated by the KSEN card of MCNP6 code, and also read the covariance matrices generated by the NJOY2021 code.

- The python script pre and post multiplies the covariance matrices by the sensitivity matrix and he transposes sensitivity matrix using the sandwish rule (Eq.(5)) to compute the uncertainties in k_{eff}.

- Then, the sensitivity of reactivity coefficients resulted from the perturbations caused by insertion of control rods are calculated using Eq.(4) for the two cores.

- Finally, the uncertainties in reactivity coefficients are calculated using the sandwish formula (Eq.(5)).

Numerical Results

As mentioned before, the aim of this study is to investigate the effect of the modifications in the BEAVRS benchmark, from the first to last version, on sensitivities and uncertainties in the multiplication factors and reactivity coefficients resulting from control rods insertions. Results are elaborated in the following sections. It is worth mensiong that only significant results, of the above mensioned cross sections that affected the sensitivity and uncertainty are stated below, other results were discarded due to their insignificant values.

Sensitivities and Uncertainties in k_{eff}

The sensitivities and uncertainties in the multiplication factors are compared to study the effect of using different coolant temperature and density in the nozzle and support plate structures in addition to the effect of changing the burnable absorber design.

Figure (3) shows the energy integrated sensitivity coefficients in k_{eff} due to perturbations in cross-sections for BV1 and BV2 when all control rods are in and out.

As can be seen in Figure (3), the multiplication factor is very sensitive to ^{235}U fission-ν and fission cross-sections, where sensitivities are positive, which means that k_{eff} increases as fission-ν and fission cross-sections increase. The multiplication factor is also sensitive to ^{238}U capture cross-section, sensitivities have negative values indicating that k_{eff} decreases as ^{238}Ucapture cross-section increases.

When all control rods are out, the differences between BV1 and BV2 sensitivities come from using different coolant densities in the nozzle and support plate structures and the effect of the burnable absorber design. To explain these effects in more detail, the sensitivity profile of ^{235}U fission-ν, ^{238}U capture, and inelastic scattering should be considered when all control rods are out, as presented in Figures (4-6).

For the ^{235}U fission ν and ^{238}U capture, there are negligible differences between BV1 and BV2 sensitivities, while there are remarkable differences in ^{238}U inelastic scattering. The reason for such differences is the influence of modifications in the BV2 cores on the neutron spectrum. There are two main effects, the first effect is the higher coolant density in the nozzle and support plate structures of the BV2 model, which slightly increases the slowing-down process caused by water scattering cross-section, as a result, there will be a reduction on fast neutrons. The second effect is the burnable absorber design in the BV2 model, the water which filled the bottom part of the absorber rod (in BV1 model) is replaced by stainless steel, leading to an abundance of fast neutrons compared to the BV1 core, where the two effects work in opposite directions.

For the ^{238}U inelastic scattering, the k_{eff} sensitivities for some energy groups increase while others decrease causing an overall increment in the BV2 core integrated sensitivity.

For the ^{235}U fission-ν and ^{238}U capture, the two effects have negligible influences since the k_{eff} is more sensitive to thermal groups for both reactions. In addition, the sensitivity coefficients for the ^{235}U fission-ν and ^{238}U capture are high and such small changes in the neutron spectrum is insignificant.

When all control rods are inserted into the core, the control rods worth strongly affects the neutron spectrum, such enormous effect overcomes the coolant density and the burnable absorber design effects that were mentioned before.

Figure (7) shows the total k_{eff} uncertainties and the significant contributors caused by cross-section uncertainty of individual nuclides for the BV1 and BV2 models when all control rods are in and out.
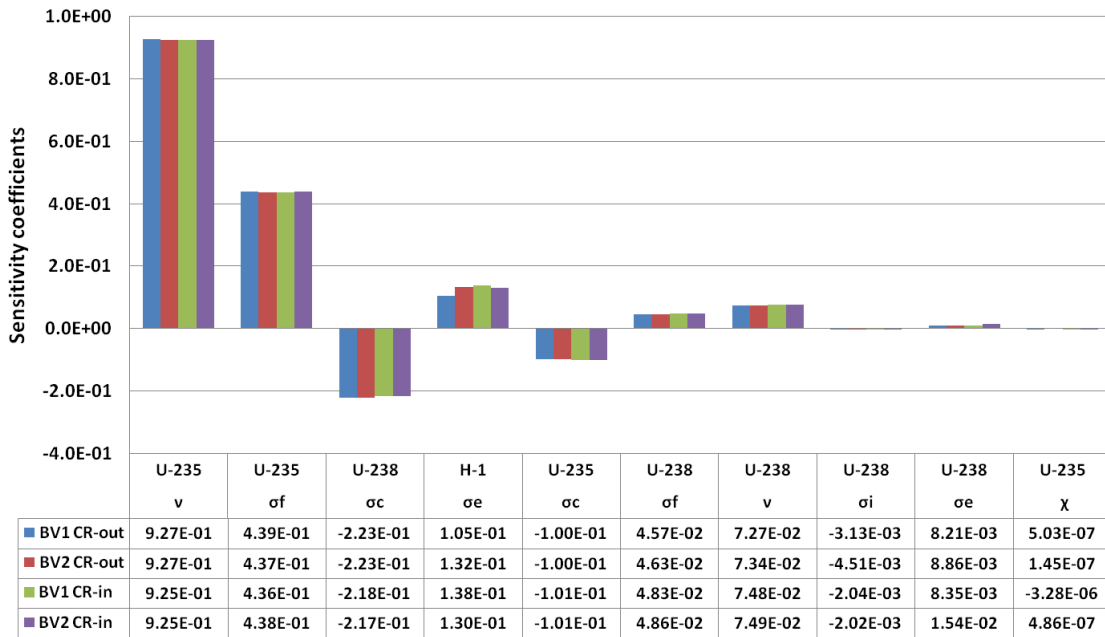

	U-235 ν	U-235 σf	U-238 σc	H-1 σe	U-235 σc	U-238 σf	U-238 ν	U-238 σi	U-238 σe	U-235 χ
BV1 CR-out	9.27E-01	4.39E-01	-2.23E-01	1.05E-01	-1.00E-01	4.57E-02	7.27E-02	-3.13E-03	8.21E-03	5.03E-07
BV2 CR-out	9.27E-01	4.37E-01	-2.23E-01	1.32E-01	-1.00E-01	4.63E-02	7.34E-02	-4.51E-03	8.86E-03	1.45E-07
BV1 CR-in	9.25E-01	4.36E-01	-2.18E-01	1.38E-01	-1.01E-01	4.83E-02	7.48E-02	-2.04E-03	8.35E-03	-3.28E-06
BV2 CR-in	9.25E-01	4.38E-01	-2.17E-01	1.30E-01	-1.01E-01	4.86E-02	7.49E-02	-2.02E-03	1.54E-02	4.86E-07

Fig. (3): The integrated sensitivities in k_{eff} for BV1 and BV2

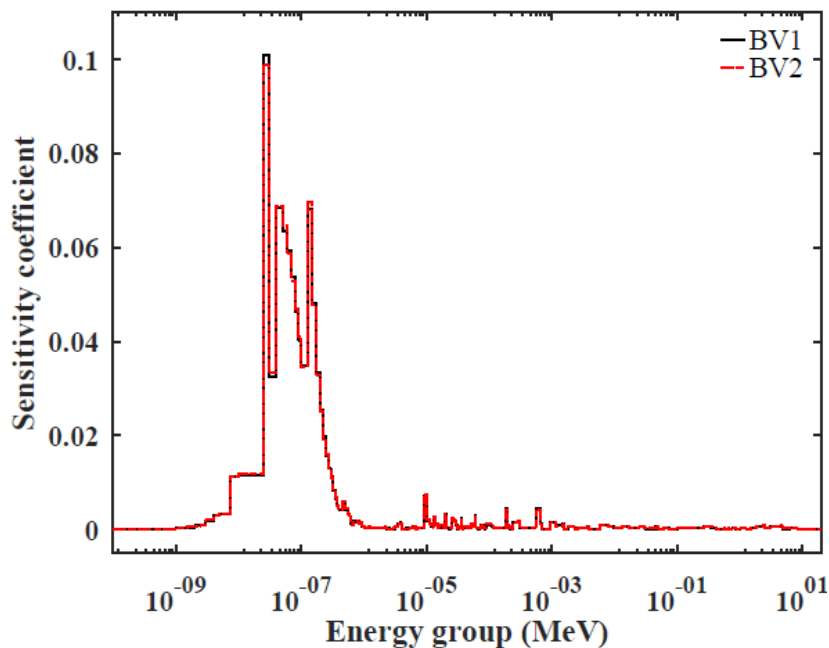**Fig. (4): Sensitivities in k_{eff} to ^{235}U fission-ν for BV1 and BV2 (CRs out)**

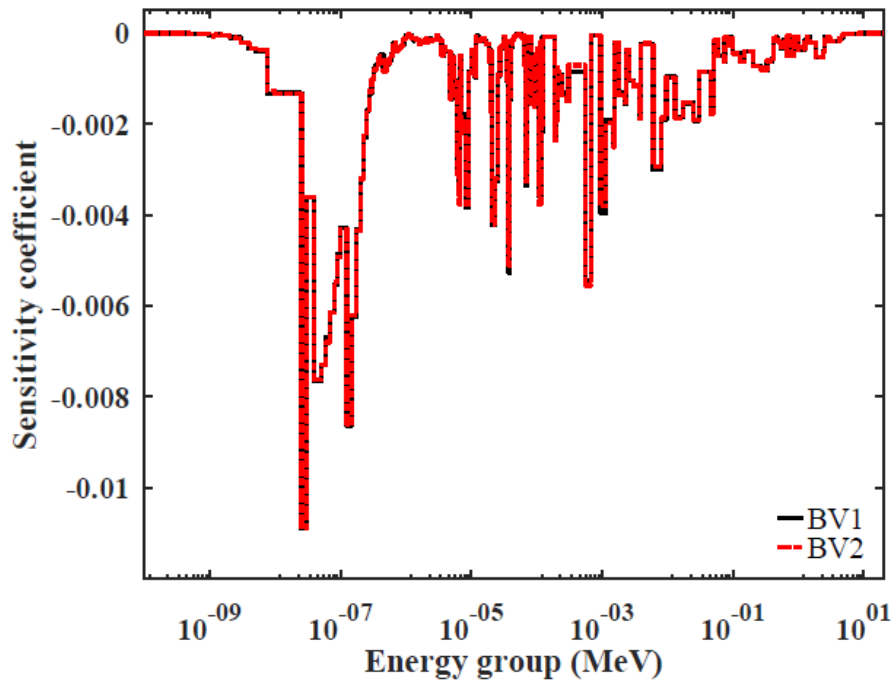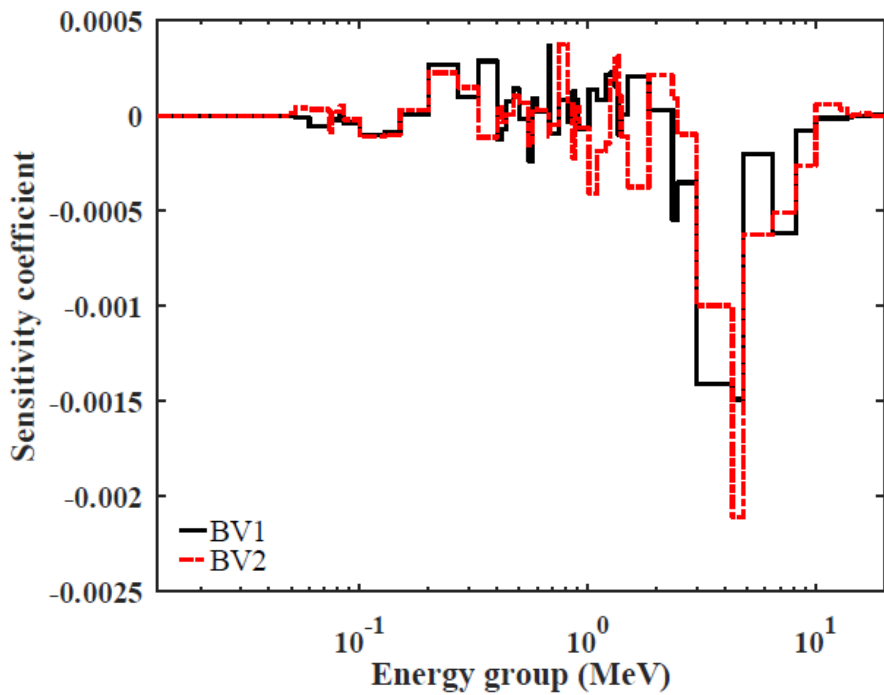**Fig. (5): Sensitivities in k_{eff} to ^{238}U capture for BV1 and BV2 (CRs out)**

Fig. (6): Sensitivities in k_{eff} to ^{238}U inelastic for BV1 and BV2 (CRs out)

When all control rods are out, the total uncertainties for BV1 and BV2 models are 0.79 and 0.80 Δk/k %, respectively. The total uncertainty slightly decreased to 0.78 Δk/k % for both models when all control rods are in. The main contributors to the uncertainties are the ^{235}U fission-ν followed by ^{238}U capture and ^{235}U capture, and fission cross-sections since k_{eff} is very sensitive to these reactions.

The ^{1}H elastic scattering has no contribution although its sensitivity is high (as seen in Figure 3), this is because the relative standard deviation ^{1}H elastic is very small. Even though, the ^{235}U fission-χ sensitivity is very small, it contributes to uncertainties because it has very high standard deviations, the same for the ^{238}U elastic and inelastic scattering. The relative standard deviation for ^{1}H elastic, ^{235}U fission-χ, ^{238}U elastic, and inelastic scattering are illustrated in Figures 8 (a-d).

Sensitivities and Uncertainties in reactivity

 Now, the influence of the modifications in the control rods designs is studied by comparing the sensitivity and uncertainty of reactivities resulting from control rods insertions. In Figure (9), the absolute value of energy-integrated sensitivity coefficients in reactivities for BV1 and BV2 models due to cross-section perturbations are explained.

Based on Eq.(4), the sensitivities in reactivity are calculated from the differences between the k_{eff} sensitivities of the two states (control rods in and out), accordingly, the BV1 model is very sensitive to the ^{1}H elastic scattering cross-section as a result of the large difference in the k_{eff} sensitivities when

control rods are in and out. This difference does not occur in the BV2 model because the slight increase in ^{1}H scattering due to the higher coolant density in the nozzle and support plate structures partially compensated the sharp decrease due to control rods insertion.

Some reactions, such as ^{238}U elastic and inelastic scattering, have the opposite behavior where the sensitivities in reactivities for the BV2 model are much greater than the corresponding sensitivities for the BV1 model. This is because of the larger differences between the k_{eff} sensitivities of the two states for the BV2 model as explained before.

Figure (10) illustrates the uncertainties in reactivities due to control rods insertion for both BV1 and BV2 models. The total uncertainties in reactivates for the BV2 model is greater than the the corresponding uncertainties for BV1 model, the total uncertainties are 2.28 and 1.41 Δk/k % for BV2 and BV1, respectively. The main contributors to the uncertainties in reactivities are the ^{238}U inelastic, elastic, ^{235}U fission-χ followed by ^{235}U fission-ν and ^{238}U fission-χ.

 Although the ^{238}U inelastic, elastic, and ^{235}U fission-χ sensitivity are smaller than ^{235}U fission-ν, however, they significantly contribute to uncertainties due to the high standard deviations in their cross-sections (Figure 8) compared to ^{235}U fission-ν as shown in Figure (11).

 According to Eq. (6), whenever the difference in the k_{eff} of the two states is small (control rods are out and in), the relative variance of the reactivity is substantially greater than the individual k_{eff} variances. Consequently, the relative uncertainties in reactivity responses are inherently large.
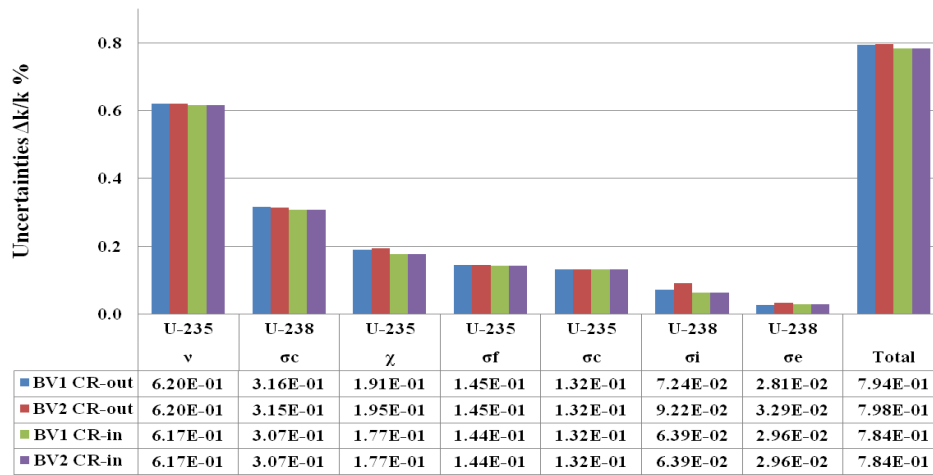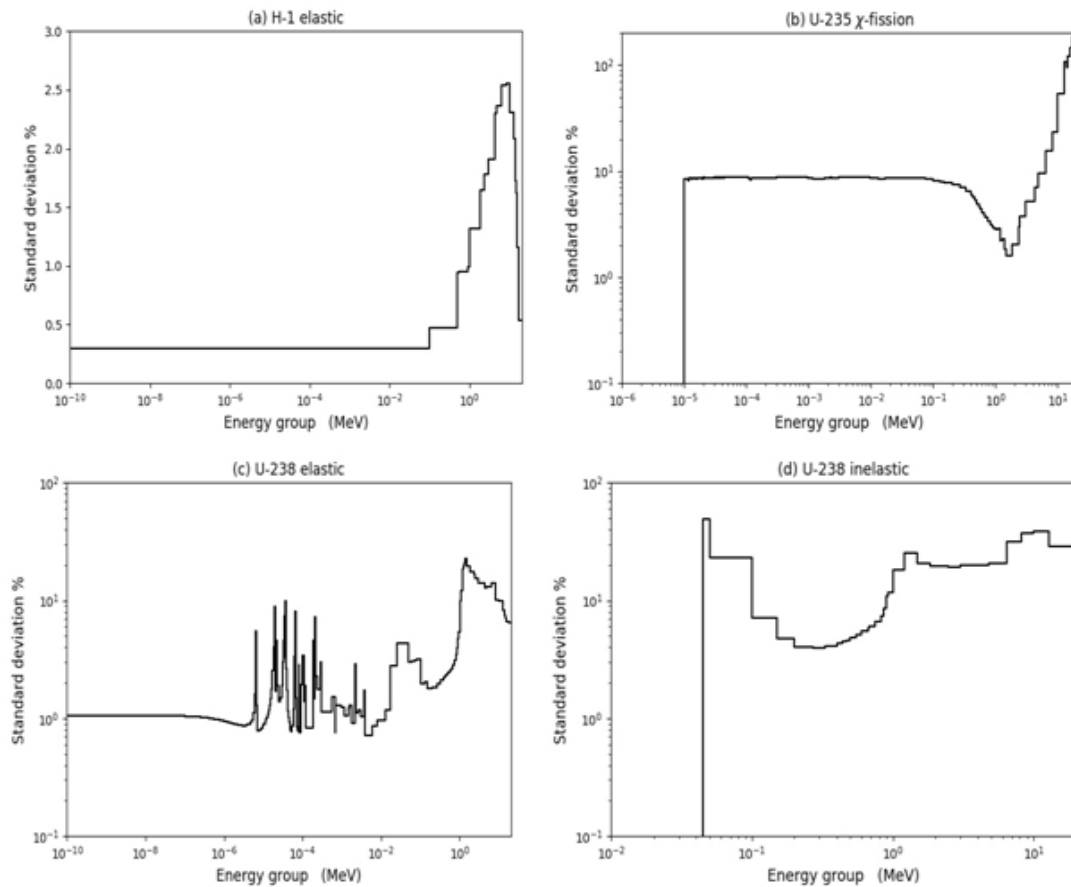
Fig. (7).The Uncertainties in k_eff for BV1 and BV2

	U-235 ν	U-238 σc	U-235 χ	U-235 σf	U-235 σc	U-238 σi	U-238 σe	Total
BV1 CR-out	6.20E-01	3.16E-01	1.91E-01	1.45E-01	1.32E-01	7.24E-02	2.81E-02	7.94E-01
BV2 CR-out	6.20E-01	3.15E-01	1.95E-01	1.45E-01	1.32E-01	9.22E-02	3.29E-02	7.98E-01
BV1 CR-in	6.17E-01	3.07E-01	1.77E-01	1.44E-01	1.32E-01	6.39E-02	2.96E-02	7.84E-01
BV2 CR-in	6.17E-01	3.07E-01	1.77E-01	1.44E-01	1.32E-01	6.39E-02	2.96E-02	7.84E-01

Fig. (8): The relative standard deviation for ^{1}H elastic, ^{235}Ufission-χ, ^{238}U elastic, and inelastic scattering

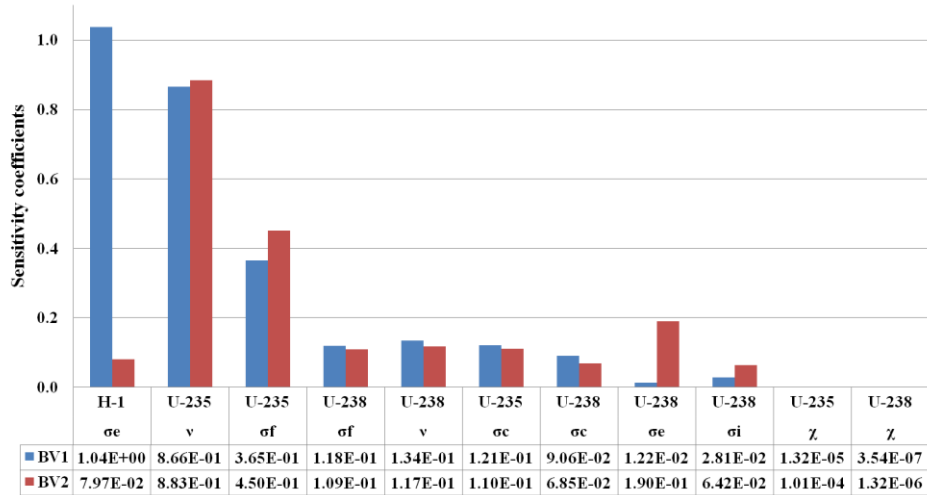|	H-1 σe	U-235 ν	U-235 σf	U-238 σf	U-238 ν	U-235 σc	U-238 σc	U-238 σe	U-238 σi	U-235 χ	U-238 χ
BV1	1.04E+00	8.66E-01	3.65E-01	1.18E-01	1.34E-01	1.21E-01	9.06E-02	1.22E-02	2.81E-02	1.32E-05	3.54E-07
BV2	7.97E-02	8.83E-01	4.50E-01	1.09E-01	1.17E-01	1.10E-01	6.85E-02	1.90E-01	6.42E-02	1.01E-04	1.32E-06

Fig. (9): The integrated sensitivities in relativities for BV1 and BV2

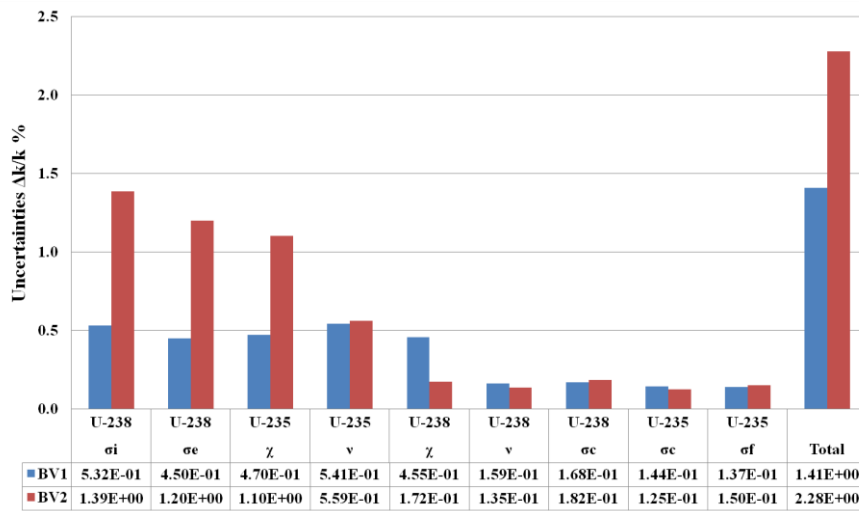|	U-238 σi	U-238 σe	U-235 χ	U-235 ν	U-238 χ	U-238 ν	U-238 σc	U-235 σc	U-235 σf	Total
BV1	5.32E-01	4.50E-01	4.70E-01	5.41E-01	4.55E-01	1.59E-01	1.68E-01	1.44E-01	1.37E-01	1.41E+00
BV2	1.39E+00	1.20E+00	1.10E+00	5.59E-01	1.72E-01	1.35E-01	1.82E-01	1.25E-01	1.50E-01	2.28E+00

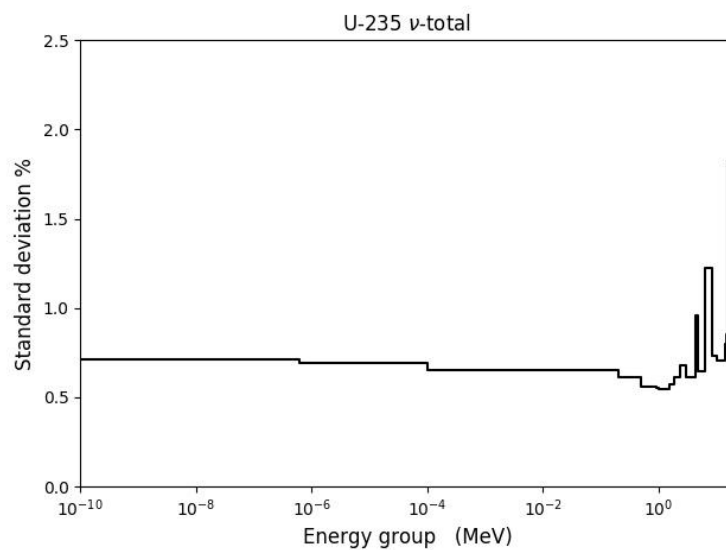**Fig. (10): The Uncertainties in reactivity for BV1 and BV2**

Fig. (11): The relative standard deviation for U-235fission-ν

Conclusions

The sensitivity and uncertainty due to model modifications in the BEAVRS benchmark were evaluated. The first and last core designs of the benchmark were simulated using MCNP6. The sensitivity coefficient was estimated using the KSEN card that utilizes the adjoint method. NJOY2021 was used to produce the covariance matrix required to estimate uncertainty.

It was found that the modification of the upper and lower structures of the BV2 model, as well as burnable poison design, had a significant effect on the sensitivity of the multiplication factor, where the multiplication factor is very sensitive to ^{235}U fission-ν, fission, and ^{238}U capture cross-sections. The main contributors to the k_{eff} uncertainties wre the ^{235}U fission- ν followed by ^{238}U capture and ^{235}U capture, and fission cross-sections.

In the BV1 model, the reactivity was very sensitive to the ^{1}H elastic scattering cross-section as a result of the large difference in the k_{eff} sensitivities. The total uncertainties in reactivity for BV2 is 62.0% , greater than that of the BV1 model, due to the effect of using higher coolant density in the nozzle and support plate structures in addition to the effect of the burnable absorber designs in the BV2 model. The main contributors to the uncertainties in reactivities were the ^{238}U inelastic, elastic, ^{235}U fission-χ uncertainties which is attributed to the high standard deviations in their cross-sections.

References

1. MIT Computational Reactor Physics Group, (2013) "BEAVRS benchmark for evaluation and validation of reactor simulations", Rev. 1.1.1. Cambridge, UK:MIT CRPG.

2. MIT Computational Reactor Physics Group, (2017), "BEAVRS benchmark for evaluation and validation of reactor simulations", Rev. 2.0.1. Cambridge, UK:MIT CRPG.

3. MIT Computational Reactor Physics Group, (2018), "BEAVRS benchmark for evaluation and validation of reactor simulations", Rev. 2.0.2. Cambridge, UK:MIT CRPG.

4. D.B. Pelowitz, (2013), "MCNP6 User's Manual Version 1.0, Los Alamos National Laboratory report, LA-CP-13-00634, Rev. 0.

5. R. E. MacFarlane, et. al. (2019), "The NJOY Nuclear Data Processing System, Version 2016", LA-UR-17-20093, updated October 2019. https://www.njoy21.io/NJOY21/.

6. D. G. Cacuci, (2003), "Sensitivity and Uncertainty Analysis", Theory, Vol. 1. Chapman& Hall/CRC, Boca Raton.

7. C.J. Diez , O. Buss, et al., (2015), "Comparison of nuclear data uncertainty propagation methodologies for PWR burn-up simulations", Annals of Nuclear Energy, 77 (101–114).

8. P. Reuss. (2008), "Neutron Physics". EdP Sciences, France.

9. B.C.Kiedrowski, (2013), "MCNP6.1 k-Eigenvalue Sensitivity Capability: A User's Guide", Los Alamos National Laboratory report, LA-UR-13-22251.

10. M. L. Williams, (2007), "Sensitivity and Uncertainty Analysis for Eigenvalue-Difference Responses," Nuclear Science and Engineering, 155 (18–36).